



## **Modelling and Verification of Solid Propellant Rocket Motor Operation**

Bogdan ZYGMUNT,\* Zbigniew SURMA,  
Zbigniew LECIEJEWSKI, Krzysztof MOTYL,  
Tomasz RASZTABIGA

*Military University of Technology,  
Faculty of Mechatronics and Aerospace,  
Kaliskiego 2, 00-908 Warsaw, Poland  
\*E-mail: bogdan.zygmunt@wat.edu.pl*

**Abstract:** This paper presents a mathematical-physical model of phenomena occurring in the combustion chamber of a new solid propellant rocket motor. Due to the fact that the geometrical shape of the propellant grain has already been elaborated, the proposal for the modelling of combustion gas generation is a novelty. To solve the system of equations associated with the mathematical model, a computer programme in Turbo Pascal 7.0 was developed. For the solution of ordinary first-order differential equations, the fourth-order Runge-Kutta numerical method was applied. The main results of the completed simulations, *i.e.* changes in gas pressure,  $p$ , in the combustion chamber, and the rocket motor thrust,  $R$ , as a function of time,  $t$ , of motor operation, are shown graphically. Experimental verification of the parameters of the designed motor shows good agreement with the numerically calculated parameters.

**Keywords:** modelling of rocket motor operation, ballistic parameters, experimental verification

### **1 Introduction**

The basic type of propulsion systems for contemporary missiles used in air defence and anti-tank systems are solid propellant rocket motors. The main advantage of such a propulsion system is its readiness for immediate combat action and the possibility of long-term storage of the projectiles under various conditions. Due to the rocket propulsion system, missiles achieve supersonic

speeds with 20-100 overloads (in relation to gravitational acceleration), *i.e.* several orders smaller than for classical artillery projectiles. Thus, mechanical and electronic modules, susceptible to overloads, can be installed in the control compartment of the rocket.

An additional advantage of rocket propulsion is the possibility of shaping the propulsive impulse, *i.e.* the instantaneous value of the propulsive effort (so-called thrust) as a time function. This can be obtained by designing a suitable geometrical shape for the propulsive charge and by covering a part of the charge with a non-flammable layer (so-called bonding) that protects the charge against ignition and burning. Modern analytical tools and software allow theoretical determination of the approximate shape of the propulsive impulse for an assumed geometrical projectile of the propulsion charge, which is made of the chosen rocket propellant. Commercial software [1] can be used to complete this; also, a mathematical-physical model of the solid propellant rocket motor operation can be built using internal ballistic laws and by considering individual characteristics of the propellant charge, combustion chamber and nozzle dimensions [2-9].

The operation of a solid propellant rocket engine of a newly-developed Polish two-stage, anti-aircraft supersonic missile [10, 11] is the subject of the analysis in this paper. Starting from the required missile performance, this paper presents a physical model of the solid propellant charge of a complex (atypical) shape, a mathematical model of the rocket engine operation (in terms of thermodynamics), and computer simulations on the basis of the original SRMIB (solid rocket motor internal ballistics) software. Difficulties in modelling the rocket motor operation also arise from the double-base propellant characteristics, namely the high heat of combustion, in excess of 4500 kJ/kg. Improvements in the motor operation, made on the basis of the analysis of the motor, have been compared with the experimental results obtained from ballistic investigations made on a motor test stand for the rocket motor with the developed propellant charge.

## 2 Physical Model of Solid Propellant Charge and Combustion Chamber

The solid propellant charge of the rocket motor of the designed air-defence missile is a 28 kg grain charge in the shape shown in Figure 1. The charge can be formally separated into two parts, with different characteristic shapes:

- sleeve-shaped element 1 (non-inhibited, bright grey in Figure 1) with an external diameter of 155 mm, an internal diameter of 55 mm, and a length of 250 mm, with four perpendicular radial grooves along the whole length;

- sleeve-shaped element 2 (inhibited on its lateral and frontal surface, dark grey in Figure 1) with an external diameter of 160 mm, an internal diameter of 55 mm, and a length of 870 mm.

The geometric data, the mass of both elements of the propelling charge, and the energetic-ballistic characteristics of the propellant are given in Table 1.

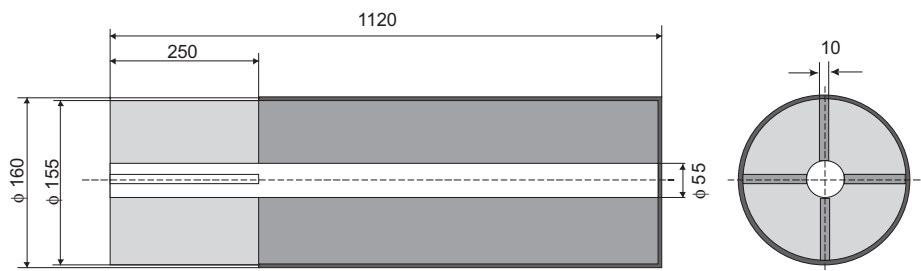


**Figure 1.** Cross-section of the propelling charge considered in this paper.

**Table 1.** Energetic and ballistic parameters of the propellant

Parameter	Symbol [Unit]	Element 1	Element 2
Force	$f_p$ [MJ/kg]	0.90	0.90
Pre-exponential in the normal burning rate law	$A$ [m/(sPa <sup>n</sup> )]	0.015	0.015
Exponential in the normal burning rate law	$n$	0.015	0.015
Ratio of specific heats (constant-pressure to constant-volume) (adiabatic exponent)	$k$	1.265	1.265
Coefficient of exponential erosive burning formula	$k_w$	$31.24 \cdot 10^{-9}$	$31.24 \cdot 10^{-9}$
Exponent of exponential erosive burning formula	$m$	3.1	3.1
Coefficient of linear erosive burning formula	$k_v$	0.006	0.006
Limiting velocity of gas in combustion chamber	$w_{gr}$ [m/s]	150	150
Shape coefficients of propellant grain	$\chi$	1.7486	0.590
	$\lambda$	-0.4609	0.7629
	$\mu$	0.0326	-0.0682
Propellant density	$\rho_p$ [kg/m <sup>3</sup> ]	1600	1600
Initial area of propellant charge	$s_0$ [dm <sup>2</sup> ]	25.94	15.23
Initial cross-sectional area of charge	$s_{cs0}$ [dm <sup>2</sup> ]	-	1.649
Propellant mass	$m_p$ [kg]	5.80	22.96
Combustion chamber filling coefficients	$a$	0.3	0.3
	$b$	5	5
Length of propellant	$l$ [m]	0.250	0.870

As presented in Table 1, the geometric characteristics of the propellant grain (elements 1 and 2) allowed us to specify the intensity of the flow of gases into the free volume of the combustion chamber and thus the gas pressure in the combustion chamber and the rocket thrust. This was made possible by determining the variation of the relative mass,  $\psi$ , of the propellant grain and the relative combustion surface,  $\sigma$ , as a function of the relative thickness of the burning layer (web size),  $z$  according to the relations given below. The values of the coefficients  $\chi$ ,  $\lambda$ ,  $\mu$  are given in Table 1.

$$\psi(z) = \chi z (1 + \lambda z + \mu z^2) \quad (1)$$

$$\sigma(z) = 1 + 2\lambda z + 3\mu z^2 \quad (2)$$

Graphs showing the variability of  $\psi(z)$  and  $\sigma(z)$  are presented in Figures 2 and 3.

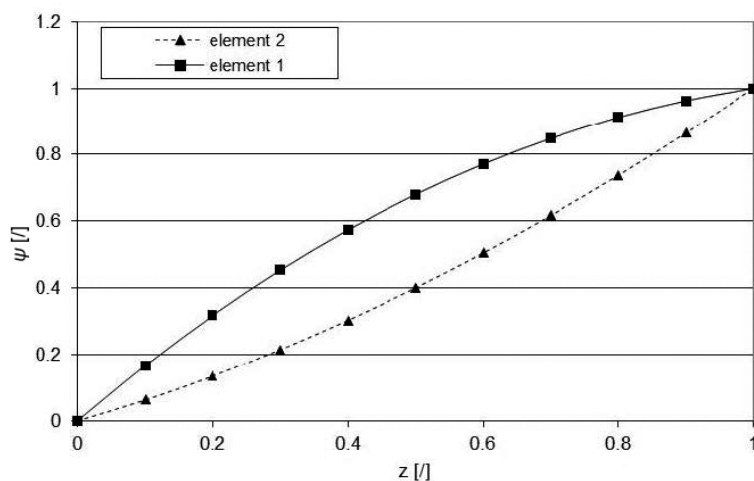


**Figure 2.** Variability of  $\psi(z)$  for both elements of the propelling charge.

Analysis of the graphs presented in Figures 2 and 3 showed a strongly degressive combustion of element 1 and a strongly progressive combustion of element 2. The methods for experimentally determining the erosion function coefficients are described in paper [13]. The basic geometric dimensions of the combustion chamber and nozzle, and the characteristics of the igniter are presented in Tables 2 and 3. Due to the relatively short operating time of the rocket motor, the ideal conditions of gas outflow were applied in the calculations.

This assumption results in the values of coefficients  $\varphi_1$  and  $\varphi_2$  being equal 1.

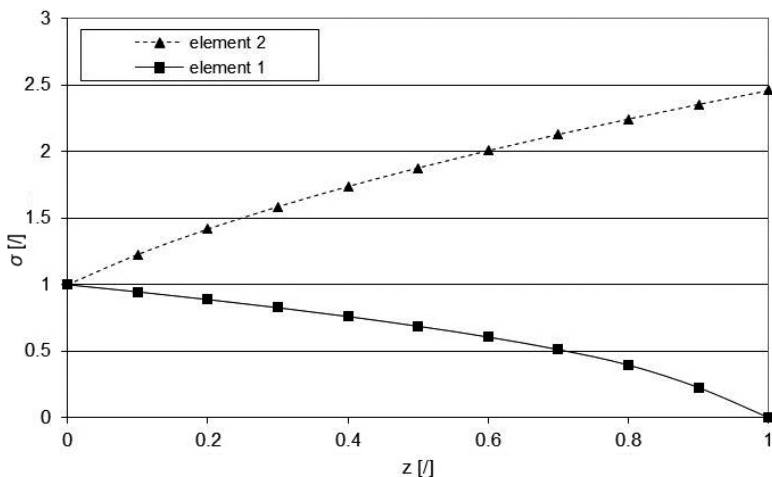


**Figure 3.** Variability of  $\sigma(z)$  for both elements of the propelling charge.

**Table 2.** Characteristics of the combustion chamber and the nozzle

Minimum (critical) diameter of nozzle	$d_m$ [mm]	40
Minimum cross-section area of nozzle	$F_m$ [dm <sup>2</sup> ]	0.1257
Inside diameter of combustion chamber	$D_c$ [mm]	160
Cross-sectional area of combustion chamber	$F_c$ [dm <sup>2</sup> ]	2.0106
Volume of combustion chamber	$V_c$ [dm <sup>3</sup> ]	22.94
Velocity loss coefficient	$\varphi_1$	1
Expenditure loss coefficient	$\varphi_2$	1

**Table 3.** Characteristics of the igniter (made of black powder)

Force	$f_i$ [MJ/kg]	0.28
Co-volume	$a_i$ [m <sup>3</sup> /kg]	$0.5 \cdot 10^{-3}$
Mass	$m_i$ [g]	33

### 3 Mathematical Model of the Rocket Motor Operation

The phenomena that take place during a solid propellant rocket motor operation can be described using the fundamental laws of physics and thermodynamics, taking into account the specific operation of the considered system. The basic

relations of the mathematical model are a balanced equation for the mass of the gases in the combustion chamber, an equation for propellant gas inflow, and an equation for the rocket motor thrust [12, 13]. The parameters appearing in the equations of the mathematical model of the operation of a solid propellant rocket motor (not given in Tables 1-3) are:

$d$  – internal diameter of element 2;

$D$  – external diameter of element 2;

$e_1, e_2$  – thickness of burned layer of element 1 and element 2, respectively;

$K_0$  – adiabatic exponent function;

$m$  – mass of gas in the combustion chamber;

$m_{in}$  – mass of gas flowing into the free volume of the combustion chamber;

$m_{out}$  – mass of gas flowing out of the combustion chamber through the nozzle;

$p$  – pressure of gas in the combustion chamber;

$s_1, s_2$  – instantaneous burning area of element 1 and element 2, respectively;

$t$  – time;

$u_1, u_2$  – burning rate of elements 1 and 2, respectively;

$V$  – free volume of the combustion chamber;

$w_{L1}, w_{L2}$  – actual maximum gas flow velocity for elements 1 and 2, respectively;

$z$  – relative thickness of the combustible layer (web size) of element 2;

$s_{cs2}$  – relative combustion cross-section surface of element 2;

$\psi_1, \psi_2$  – relative mass of the combusted elements 1 and 2, respectively.

The instantaneous gas mass balance in the combustion chamber may be expressed as:

$$dm_{in} - dm_{out} = dm \quad (3)$$

where:

$$dm_{in} = \rho_{p1}s_1u_1dt + \rho_{p2}s_2u_2dt$$

$$dm_{out} = \varphi_2 \frac{K_0(k)}{\sqrt{\chi f_p}} F_m p dt$$

$$m = \frac{pV}{\chi f_p} \quad dm = \frac{dpV + pdV}{\chi f_p} - \frac{d\chi}{\chi} m \quad Vd = s_1de_1 + s_2de_2$$

Based on the above relationships, the pressure variation in the rocket motor chamber as a function of time is predicted using the following equation:

$$\frac{dp}{dt} = \frac{1}{V} \left[ (\rho_{p1}s_1u_1 + \rho_{p2}s_2u_2)\chi f_p - \left( \varphi_2 K_0(k) F_m \sqrt{\chi f_p} + s_1u_1 + s_2u_2 - V \frac{d\chi}{\chi dt} \right) p \right] \quad (4)$$

The mass of gas generated by combustion of the propellant charge is given as:

- for element 1

$$\frac{d\psi_1}{dt} = \frac{\rho_{p1}}{m_{p1}} s_1 u_1(p, w_{L1}) \quad s_1 = s_{01} \sqrt{1 + 4 \frac{\lambda_{11}}{\chi_{11}} \psi_1} \quad (5)$$

- for element 2

$$\frac{d\psi_2}{dt} = \frac{\rho_{p2}}{m_{p2}} s_2 u_2(p, w_{L2}) \quad s_2 = s_{02} \sqrt{1 + 4 \frac{\lambda_{12}}{\chi_{12}} \psi_2} \quad (6)$$

The rocket thrust was calculated using:

$$R = 1.5 \cdot F_m \cdot p \quad (7)$$

Additional dependences express:

- a) the heat loss factor (for element 2)

$$\chi = 1 - \frac{a}{1 + b\psi_2} \quad \frac{d\chi}{dt} = \frac{ab}{(1 + b\psi_2)^2} \frac{d\psi_2}{dt} \quad (8)$$

- b) the burning rate law (assuming that the initial temperature of the propellant is equal to the normal temperature)

- for element 1

$$u_1(p, w_{L1}) = f(p) \cdot \varphi(w_{L1}) \quad (9)$$

- for element 2

$$u_2(p, w_{L2}) = f(p) \cdot \varphi(w_{L2}) \quad (10)$$

where:

$f(p)$  – pressure formula of the burning rate law,  $f(p) = Ap^n$

$\varphi$  – erosion formula of the burning rate law; it is possible to express this as a linear or exponential expression [13]

$$- \varphi(w_{L1}) = 1 + k_w w_{L1}^m \quad \text{or} \quad \varphi(w_{L1}) = 1 + k_v (w_{L1} - w_{gr})$$

$$- \varphi(w_{L2}) = 1 + k_w w_{L2}^m \quad \text{or} \quad \varphi(w_{L2}) = 1 + k_v (w_{L2} - w_{gr})$$

- c) the instantaneous maximum gas flow velocity

- for element 2

$$w_{L2} = \varphi_1 K_0(k) \sqrt{\chi f_p} \cdot \frac{F_m}{F_{p2}} \quad (11)$$

- for element 1

$$w_{L1} = \frac{l_1}{l_1 + l_2} \cdot w_{L2} \quad (12)$$

- d) the instantaneous cross-sectional flow channel of the combustion chamber (with regard to element 2)

$$F_{p2} = F_c - S_{cs02}\sigma_{cs2} \quad (13)$$

where:  $\sigma_{cs2} = 1 - \frac{2d}{D+d}z - \frac{D-d}{D+d}z^2$

- e) the instantaneous free volume of the combustion chamber

$$V = V_c - \frac{m_{p1}}{\rho_{p1}}(1 - \psi_1) - \frac{m_{p2}}{\rho_{p2}}(1 - \psi_2) \quad (14)$$

- f) the ignition pressure

$$p_i = \frac{f_i \cdot m_i}{V_c - \frac{m_{p1}}{\rho_{p1}} - \frac{m_{p2}}{\rho_{p2}} - \alpha_i \cdot m_i} \quad (15)$$

The initial conditions for the calculation were as follows:  $t = t_0 = 0$ ,  $\psi_1 = \psi_2 = 0$ ,  $\chi = \chi(t_0)$ ,  $p = p_i$ .

## 4 Simulation of the Rocket Motor Operation

In order to solve the equations of the mathematical model as presented in Section 3, the computer programme, SRMIB, in Turbo Pascal 7.0 was developed. The fourth-order Runge-Kutta numerical method was applied for the solution of the ordinary first-order differential equations. For the calculations, geometrical data of the combustion chamber, nozzle, and propellant charge, as well as the energetic-ballistic characteristics of the propellant (including the coefficients of the pressure and erosion functions) and igniter are the same as given in Tables 1-3. The simulations also assumed the following initial conditions:  $t = t_0 = 0$ ,  $\psi_1 = \psi_2 = 0$ ,  $\chi = \chi(t_0)$ ,  $p = p_i = 1.65$  MPa.

The main results of the simulations, namely, the pressure,  $p$ , of the gases in the combustion chamber and the rocket thrust,  $R$ , are shown in Figures 4 and 5, where the influence of a form of the erosion function used on the main ballistic characteristics ( $p$ ,  $R$ ) is presented.



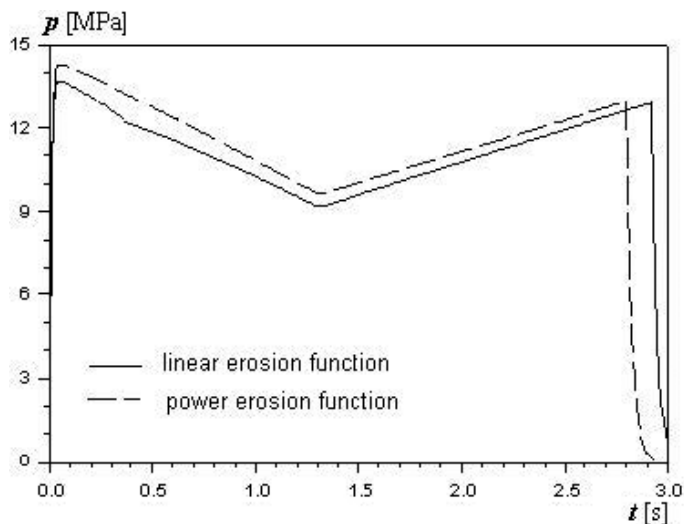


**Figure 4.** Pressure vs. time in the combustion chamber. The calculations were performed taking into account the linear (solid line) or power (dotted line) erosion formula of the burning rate law.

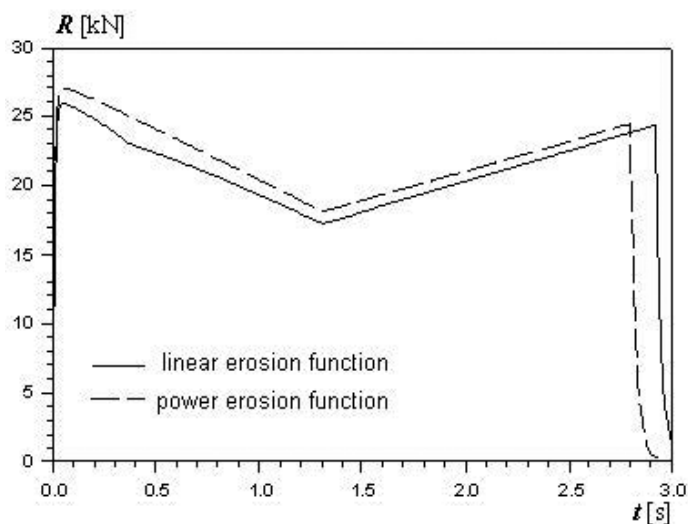


**Figure 5.** Rocket thrust vs. time. The calculations were performed taking into account the linear (solid line) or power (dotted line) erosion formula of the burning rate law.

## 5 Experimental Verification of the Ballistic Parameters of the Rocket Motor

The propellant charges were made of double-base propellant using an extrusion method. The final shape of the charges, after deposition of an inhibitor layer, was obtained by mechanical treatment. Figure 6 shows the propellant charges of the model series that were made according to the assumptions resulting from the theoretical analysis (Sections 2 and 3). The ballistic investigations of the propellant charges in metal combustion chambers were made at ambient temperature. Ballistic tests were carried out using HBM Inc. (USA) equipment. P6A pressure transducers and a C2 force gauge were used to measure the pressure in the rocket motor chamber and the thrust of the rocket motor, respectively. A computer equipped with dedicated software Catman 32 v.6 (HBM Inc.) was used to record and process the signals from the sensors. Several tests (six successful) were conducted to confirm the repeatability of the ballistic parameters of the rocket motor lot. The distribution of the results did not exceed 5%.



**Figure 6.** View of a lot of double-base propellant charges for the ballistic tests [14].

The results from the ballistic tests of the designed rocket motor are shown in Figure 7. It can be observed that satisfactory qualitative and quantitative agreement exists between the experimental and simulation results for the pressure and thrust *vs.* time. The difference between the maximum and minimum values of the measured ballistic parameters during rocket motor operation, did not exceed

20%, which has a positive effect on the sufficient strength of the rocket motor chamber and the kinematic parameters of the driven missile.

The mass of the ignition charge was chosen experimentally. The igniter mass significantly influences the initial run of the rocket motor ballistic parameters. Too large an ignition mass (black powder) in the igniter increases the pressure in the combustion chamber, which is unfavourable for construction; too small an ignition mass delays or even fails to cause ignition of the propellant charge, especially at low temperatures. Figure 8 shows the initial runs of the ballistic parameters of the motor for various masses of the powder charge of the igniter, *i.e.* 33, 40, and 50 g.

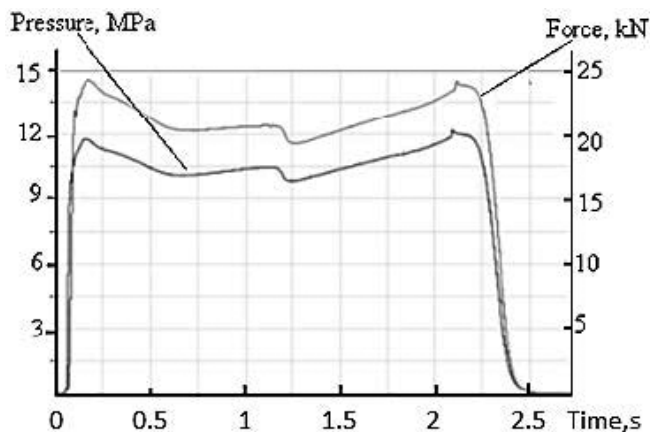


**Figure 7.** Thrust and pressure vs. time, recorded during the ballistic test.

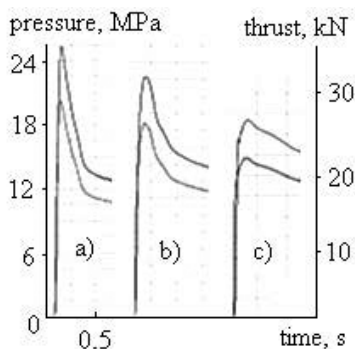


**Figure 8.** Shape of the initial part of the thrust and pressure vs. time runs recorded for different masses of the igniter charge: a) 50 g, b) 40 g, c) 33 g, of black powder.

## 6 Conclusions

The objective of the ballistic analysis was a rocket motor containing 28 kg of a complex propellant grain, made of double-base propellant with a heat of combustion exceeding 4500 kJ/kg.

For the elaborate shape of the propellant grain, the values of the geometric characteristics,  $\chi$ ,  $\lambda$ , and  $\mu$ , were calculated, and the diagrams of the variability of the functions,  $\psi(z)$  and  $\sigma(z)$ , for both elements of the rocket propellant charge were discussed. From the analysis of these diagrams, it was determined that the burning of element 1 is degressive in nature and the burning of element 2 is highly progressive in nature. The mathematical model of the rocket motor operation was presented, in which the analysed shape of the propellant grain was used. The results of the completed simulations, shown in the form of diagrams of gas pressure  $p$  in the combustion chamber and the rocket motor thrust  $R$  as a function of motor operation time  $t$ , are presented. Experimental verification of the parameters of the designed motor shows good agreement with the theoretically calculated parameters.

The developed computer programme allows for the analysis of the rocket motor operation, especially for the determination of the pressure changes,  $p(t)$ , of the gases in the combustion chamber, and the thrust,  $R(t)$ , of the rocket motor, with regard to changes in the following conditions:

- geometric dimensions of the propellant grain;
- energetic-ballistic characteristics of the propellant;
- geometric dimensions of the combustion chamber and nozzle;
- initial conditions of ignition.

## References

- [1] PRODAS, Arrow Tech Associates, Inc. USA, **2008**.
- [2] Coats D.E., Dunn S.S., French J.C., *Performance Modelling Requirements for Solid Propellant Rocket Motors*, Chemical Propulsion Information Agency, **2003**.
- [3] Coats D.E., French J.C., Dunn S.S., Berker D.R., Improvements to the Solid Performance Program (SPP), *39<sup>th</sup> AIAA/ASME/SAE/ASEE Joint Propulsion Conference*, Huntsville, AL, **2003**.
- [4] Coats D.E., Levine J.N., Cohen N.S., Nickerson G.R., Tyson T.J., *A Computer Program for the Prediction of Solid Propellant Rocket Motor Performance*, Vol. 1, Air Force Rocket Propulsion Laboratory, **1975**.
- [5] Scippa S., Propellant Grain Design, in: *Design Methods in Solid Rocket Motors*, AGARD-LS-150 (Revised), Paris, **1988**.

- [6] Alvilli P., Buckmaster J., Jackson T.L., Short M., Ignition-transient Modelling for Solid Propellant Rocket Motors, *36<sup>th</sup> AIAA/ASME/SAE/ASEE Joint Propulsion Conference and Exhibit*, Huntsville, AL, **2000**.
- [7] Alvilli P., Tafti D., Najjar F., The Development of an Advanced Solid Rocket Flow Simulation, Program ROCFLO, *38<sup>th</sup> AIAA Aerospace Sciences Meeting and Exhibit*, Reno, NV, **2000**.
- [8] Willcox M.A., Brewster M.Q., Tang K.C., Stewart D.S., Kuznetsov I., Solid Rocket Motor Internal Ballistics Simulation using Three-dimensional Grain Burnback, *J. Propul. Power*, **2007**, 23, 3.
- [9] Terzic J., Zecevic B., Baskarad M., Catovic A., Serdarevic-Kadic S., Prediction of Internal Ballistic Parameters of Solid Propellant Rocket Motors, *Problems of Mechatronics. Armament, Aviation, Safety Engineering*, **2011**, 2(4), 7-26.
- [10] Zygmont B., Motyl K., Machowski B., Makowski M., Olejniczak E., Rasztabiga T., Theoretical and Experimental Research of Supersonic Missile Ballistics, *Bull. PAS – Technical Science*, **2015**, 63(1), 229-233.
- [11] Rasztabiga T., Motyl K., Zygmont B., Kaźmierczak R., The Concept of a Two-stage Supersonic Missile Design (in Polish), *Problems of Mechatronics. Armament, Aviation, Safety Engineering*, **2014**, 5(3), 51-68.
- [12] Torecki S., *Rocket Engines* (in Polish), MKL, Warszawa, **1984**.
- [13] Razdan K.M., Kuo K.K., Erosive Burning of Solid Propellants, Fundamentals of Solid Propellant Combustion, (Kuo K.K., Summerfield M., Eds.), *Progress in Astronautics and Aeronautics*, vol. 90, AIAA, **1984**.
- [14] Drabik Z., Rasztabiga T., Rocket Motor with Composite Combustion Chamber (in Polish), *Problems of Mechatronics. Armament, Aviation, Safety Engineering*, **2015**, 6(3), 71-83.